Provided for non-commercial research and education use.
Not for reproduction, distribution or commercial use.

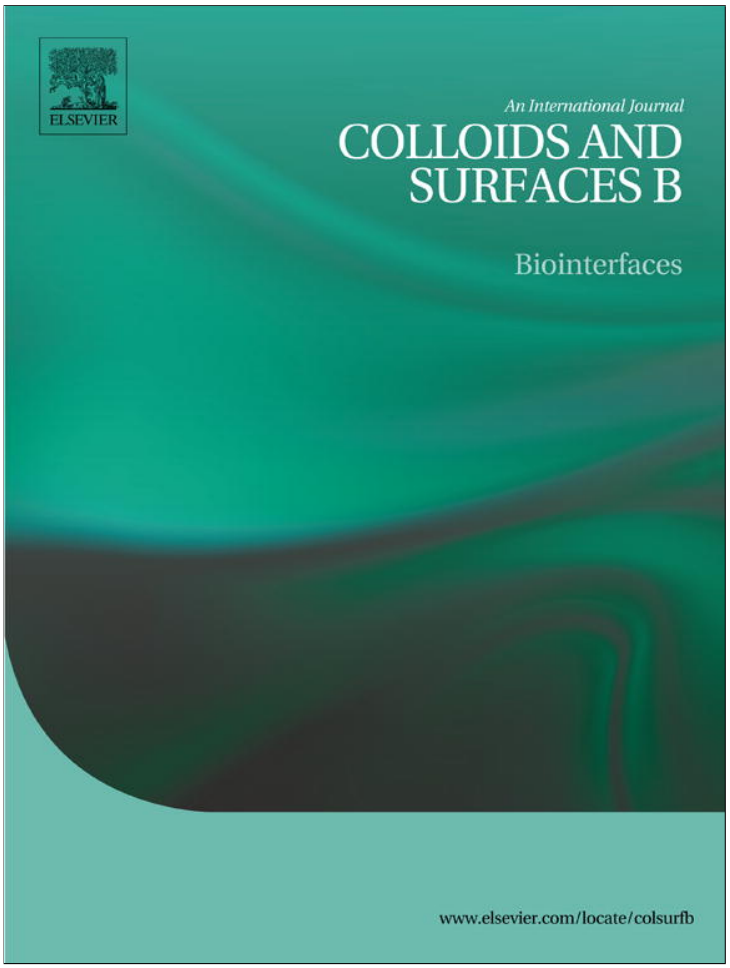

(This is a sample cover image for this issue. The actual cover is not yet available at this time.)

This article appeared in a journal published by Elsevier. The attached copy is furnished to the author for internal non-commercial research and education use, including for instruction at the authors institution and sharing with colleagues.

Other uses, including reproduction and distribution, or selling or licensing copies, or posting to personal, institutional or third party websites are prohibited.

In most cases authors are permitted to post their version of the article (e.g. in Word or Tex form) to their personal website or institutional repository. Authors requiring further information regarding Elsevier's archiving and manuscript policies are encouraged to visit:

http://www.elsevier.com/copyright

Author's personal copy

Colloids and Surfaces B: Biointerfaces 105 (2013) 319–327

Contents lists available at SciVerse ScienceDirect

Colloids and Surfaces B: Biointerfaces

journal homepage: www.elsevier.com/locate/colsurfb

Amaranth proteins foaming properties: Adsorption kinetics and foam formation—Part 1

Agustín J. Bolontrade, Adriana A. Scilingo, María C. Añón*

Centro de Investigación y Desarrollo en Criotecnología de Alimentos (CIDCA), Facultad de Ciencias Exactas, Universidad Nacional de La Plata, CCT, La Plata, CONICET (Consejo Nacional de Investigaciones Científicas y Técnicas), Calle 47 y 116, 1900 La Plata, Argentina

ARTICLE INFO

Article history:
Received 4 May 2012
Received in revised form
17 December 2012
Accepted 19 December 2012
Available online xxx

Keywords:
Amaranth proteins
Interface air/water
Foam formation

ABSTRACT

This work has focused on the study of the relationships between the structural changes in proteins of amaranth under different conditions of pH and ionic strength and the ability to form foam, also taking into consideration the kinetics of adsorption of proteins at the interface. Results showed that treatment at pH 2.0 significantly improves the foaming properties of amaranth proteins. The structural studies performed indicate that amaranth proteins at acidic pH are denatured, dissociated and undergo partial hydrolysis due to the existence of an endoprotease. They also present a lower content of β-sheet and random coil secondary structures. Diffusion–adsorption studies of proteins at the air:water interface allowed to determine that the acidic pH favors adsorption thereof (higher values of k_{diff} and k_a) and reduces the need for a rearrangement (higher values of γ_r). The interfacial behavior of amaranth proteins is a direct consequence of the structural changes they undergo at acidic pH, changes that also were reflected on the increased foaming capacity (higher v_o) thus forming more dense and homogeneous foams. The behavior of the soluble proteins as surfactants was not altered by the presence of protein aggregates and insoluble proteins.

© 2013 Elsevier B.V. All rights reserved.

1. Introduction

Food demand in the growing world population has prompted the search for new protein sources [1]. In this context, vegetable proteins are emerging as a promising alternative to replace partially animal for human protein [2]. Amaranth seeds have a high content of storage proteins (14–19%) [3], whose aminoacid composition is rich in lysine and methionine, two limiting aminoacids in cereals and legumes, respectively [4,5]. In the recent years different researchers have found some biological activities of proteins and/or peptides of amaranth [6,7], making this pseudocereal a more interesting source for use in nutraceutical products and/or functional food ingredients.

The role of proteins as surfactants in food dispersions – emulsion and foams – has been studied by many authors [8–10]. The knowledge of interfacial properties of proteins, in this particular case, amaranth's proteins, is necessary for its use as foam functional foods. The expression of the surface activity of proteins is the result of several processes that result in the diffusion of the protein from bulk solution to the interface. This activity is related to the physical, chemical and conformational characteristics of the macromolecules, which are affected by extrinsic factors such as pH, ionic strength, temperature, etc. [11].

Recently, Ventureira et al. [12] have studied the interfacial and emulsifying properties of amaranth proteins at acidic and alkaline pHs. The results obtained by these authors indicate that amaranth proteins at acidic pH are more soluble, have a better activity at the oil:water interface and are capable of forming stable emulsions.

In this context, the aim of this study was to obtain additional experimental information about structural characteristics of amaranth proteins in solution and to provide new insights on the kinetics of diffusion, adsorption and rearrangement at the air:water interface under different conditions of pH and ionic strength (μ). These structural and interfacial characteristics were related to parameters indicative of the formation of amaranth proteins foams, in order to evaluate its potential application in the development and improvement of foam functional foods.

2. Materials and methods

2.1. Plant materials and flour preparation

Seeds of *Amaranthus hypochondriacus* (cultivar 9122) were obtained from Estación Experimental del Instituto Nacional de Tecnología Agropecuaria (INTA), Anguil, La Pampa, Argentina. Seeds were ground and sieved through a 0.092 mm mesh at Facultad de

* Corresponding author at: CIDCA, Calle 47 y 116, 1900 La Plata, Argentina. Tel.: +54 221 4249287; fax: +54 221 4254853.
E-mail address: mca@biol.unlp.edu.ar (M.C. Añón).

0927-7765/$ – see front matter © 2013 Elsevier B.V. All rights reserved.
http://dx.doi.org/10.1016/j.colsurfb.2012.12.039

Author's personal copy

Ciencias Agrarias y Forestales, Universidad Nacional de La Plata. The resulting flour was defatted with hexane at 4 °C for 24 h (100 g/l suspension) under continuous stirring, dried at room temperature and stored at 4 °C until used. The protein content (19.8 ± 0.2% wet basis) was determined by the Kjeldahl's method [13], $N \times 5.85$ [14].

2.2. Preparation of amaranth isolates

Amaranth isolates (AI) used in this study were prepared according to Martínez and Añón [15]. Briefly, defatted flour was suspended in water (100 g/l) and the pH was adjusted to 9.0 with 2 N NaOH. The suspension was stirred for 60 min at room temperature and then centrifuged for 20 min at 9000 × *g* at 15 °C. The supernatant was adjusted to pH 5.0 with 2 N HCl and then centrifuged at 9000 × *g* for 20 min at 4 °C. The pellet was suspended in water, neutralized with 0.1 N NaOH and freeze-dried. The isolates obtained were stored at 4 °C until used. The protein content of the isolate (85 ± 1%, dry basis) was determined by the Kjeldahl's method [13], $N \times 5.85$ [14]. At least three different batches were prepared, showing similar properties.

The protein isolates were dispersed at pH 2 in 0.035 M phosphoric acid–diacid phosphate buffer, and at pH 8 in 0.035 M Tris buffer. The ionic strength (IS) was adjusted to 0.5 and 0.06 with 0.5 M NaCl, obtaining four amaranth isolates named AI pH2-highIS, AI pH8-highIS, AI pH2-lowIS and AI pH8-lowIS (Table 1).

2.3. Electrophoresis

Sodium dodecyl sulfate-polyacrylamide gel electrophoresis (SDS-PAGE). Runs were carried out in stacking and separating gels containing 40 g/l and 120 g/l acrylamide, respectively [16]. The following continuous buffer system was used: 0.375 M Tris–HCl, pH 8.8, 1 g/l SDS for the separating gel; 0.025 M Tris–HCl, 0.192 M glycine and 1 g/l SDS, pH 8.3 for the running gel, and 0.125 M Tris–HCl, pH 6.8 A solution containing 200 ml/l glycerol, 10 g/l SDS, and 0.5 g/l bromophenol blue was used as sample buffer. For runs under reducing conditions the sample buffer contained 50 ml/l of 2-mercaptoethanol (2-ME), and samples were heated for 60 s in a boiling water bath. The protein molecular mass standards were: phosphorylase b (94 kDa); bovine serum albumin (67 kDa); ovalbumin (43 kDa); carbonic anhydrase (30 kDa); trypsin inhibitor (20.1 kDa); α-lactalbumin (14.4 kDa). Gels were fixed and stained with Coomassie Brilliant Blue Stain. Gels images were analyzed with Image J in order to determine the molecular masses of the polypeptides and the relative intensity of the bands. Soluble and insoluble fractions at both pH conditions and ionic strength were analyzed by SDS-PAGE. Electrophoretic runs were repeated twice.

2.4. Differential scanning calorimetry (DSC)

Total protein fractions were analyzed by DSC according to the method of Martínez et al. [15]. Samples were prepared in the corresponding buffers. Aluminum hermetic capsules (Perkin-Elmer No. 0219-0062) were loaded with 10–15 mg of the 200 g/l dispersions and allowed to stabilize for at least 30 min at room temperature (25 °C) before testing. Runs were performed in a DSC Polymer Laboratories device (Rheometric Scientific), at a heating rate of 10 °C/min between 28 °C and 130 °C. An empty sealed double capsule was used as a reference. All experiments were conducted in triplicate.

2.5. Solubility

The solubility of isolates was analyzed by preparing 10 g/l suspensions in the corresponding buffers. The suspensions were prepared in duplicate. Samples were incubated 1 h at room temperature (25 °C) and were vortexed during 4 s every 15 min. Samples were then centrifuged at 10,000 × *g* for 15 min at room temperature. Protein content in the supernatant (*s*) was determined by the Lowry's method [17]. Colorimetric determinations were performed in duplicate. Solubility (*S*) was expressed as follows:

$$\%S = \frac{s \times 100}{\text{total protein}}$$

Total protein content was determined with the Kjeldahl's method ($N \times 5.85$).

2.6. Circular dichroism (CD)

Differences in the secondary structure of buffer-soluble proteins at pH 2.0 and 8.0, at two ionic strengths 0.06 and 0.5, were determined by measuring the absorbance of polarized light in the 190–250 far UV range. Samples were stirred 1 h at room temperature in sample-to-buffer proportions adequate to have a soluble protein concentration of 1 g/l and then centrifuged at 10,000 × *g* for 30 min at 20 °C. The supernatant was poured into a quartz measure cell with a light path length of 0.1 mm. CD measurements were carried out in a Jobin–Yvon CD6 spectropolarimeter (Jovin–Yvon SA, Longjumeaux, France). Absorbance differences were calculated and plotted versus wavelength. Samples were analyzed in duplicate and five spectra of each sample were used for analysis.

2.7. Particle size distribution

The particle size distributions were derived from the time correlation function of the light scattering intensity measured at a single scattering angle with a goniometer ALV/CGS-5022F and a multiple *tau* digital correlator ALV-5000. The light source consisted of a helium/neon laser operating at 22 mW. All the measurements were carried out at room temperature. Solutions (1 mg/ml) were prepared and filtered (pore size 22 μm) into the cells.

Number-weighted distributions of particle size were calculated from the intensity weighted distributions assuming Rayleigh scatterers [18].

2.8. Protein diffusion and adsorption – rearrangement at interface

The interfacial tension of solutions of low protein concentration (0.01 and 0.001 mg/ml) was measured by using the automated drop tensiometer (Tracker, IT-Concept, Saint-Clément Places, France). The bubble was formed in the protein solution and the surface tension over time was calculated based on changes in drop form. The diffusion coefficient (k_{diff}) was estimated applying the modified equation of Ward and Torday [19].

The adsorption of the protein to the interface and its consequent rearrangement were measured with a drop volume tensiometer (LAUDA TVT2) in the dynamic mode. A protein solution of 1 mg/ml was used in the assays, where the soluble fraction was obtained by centrifugation at 10,000 × *g* during 15 min at 25 °C. A pendant drop of solution was formed at different rates, and the interfacial tension was calculated from the volume of the drop released when gravity outweighed the counterbalance of surface tension. The experimental data were adjusted with a biphasic first order equation $\gamma(t) = \gamma_a e^{-k_a t} + \gamma_r e^{-k_r t} + \gamma_e$ [20]. The first order rate constants (k_a, k_r), and amplitudes (γ_a, γ_r) of the adsorption and rearrangement processes of the proteins in the air–water interface were estimated.

Author's personal copy

Table 1
Nomenclature, conditions of preparation, percent solubility and thermal parameters of samples. Values are presented as mean ± SD.

Samples	Buffer conditions		% solubility[a]	Thermic parameters[b]		
	pH	IS		T_d (°C)		ΔH (J/g)
AI pH8-lowIS	8	0.06	70 ± 4	70.2 ± 0.2	99 ± 1	10.51 ± 0.04
AI pH8-highIS		0.5	59 ± 1	74.6 ± 0.4	101.7 ± 0.7	8.3 ± 0.2
AI pH2-lowIS	2	0.06	87 ± 3	nd		nd
AI pH2-highIS		0.5	25.3 ± 0.4	nd		nd

nd: endotherms not detected.
[a] Assay was made in duplicated.
[b] Thermograms were obtained at least in triplicated.

2.9. Foaming properties

The foaming properties of amaranth proteins were determined by conductimetry using the method and device developed by Loisel et al. [21].

Protein dispersions (soluble and insoluble protein) or protein solutions at 1.0 mg/ml of soluble protein were prepared in the corresponding buffers. Protein solutions were obtained after centrifugation at 10,000 × g during 15 min. Protein dispersions or protein solutions were placed in the sparging chamber at the base of an acrylic column (length: 27.5 cm, internal and external diameters: 2.4 and 3.0 cm, respectively). Foam was generated by sparging nitrogen through porous G4 type glass disk with a pore size of 5–15 μm at a rate of 80 ml/min into 6 ml of the sample during 30 s. The volume of initial or residual liquid under the foam was measured by conductivity through two electrodes located in the sparging chamber. Conductivity values, as a function of time (C_t) and with reference to the conductivity of the buffered test solution (C_{init}), were used to calculate the volume of liquid in the foam (V_L): $V_L = V_{init}[1 - (C_t/C_{init})]$, where V_{init} is the volume of sample solution (6 ml) introduced into the sparging chamber [21]. Foaming capacity was estimated from the initial rate of foam formation (v_o), maximum volume of liquid in the foam (V_L), and maximal density of foam, D_{max} (with D_{max} = maximum volume of liquid in the foam/maximum volume of foam). The images were obtained with an integrated webcam (Creative, resolution 320 × 256 pixels when the bubbling finished) with an error of ±1 s capture. The images take a portion of 7.5 mm × 6 mm of the real foam. Measurements were performed in triplicate.

2.10. Statistical analysis

The least significant difference (LSD) test (after analysis of variance, ANOVA) was used to identify paired differences between means. Significance was determined at $p < 0.05$.

3. Results and discussion

3.1. Characterization of amaranth isolates

The AI pH8-lowIS exhibited two denaturation endotherms with peak temperatures of 70.2 ± 0.2 and 98.8 ± 1.1 °C, respectively (Table 1). The enthalpy associated to the process was 10.5 ± 0.04 J/g of protein. These values agree with those obtained previously by Martínez et al. [15]. Increasing of ionic strength causes a significant increase of the temperatures of denaturation ($p < 0.05$) for the two endotherms detected (Table 1). Furthermore, the enthalpy of the process decreased, a result which could be associated to the aggregation exerted at high saline concentrations. Both effects have been previously described by Arntfield and Murray [22]. Samples at pH 2.0 (AI pH2-lowIS and highIS) did not exhibit endotherms, indicating a denaturation phenomenon induced by pH.

Amaranth protein isolates were also analyzed by denaturing and reducing denaturing electrophoresis (Fig. 1). The constituent polypeptides of AI pH8 have been previously described by Martínez et al. [16]. Such polypeptides are part of the 7S, 11S and P globulins, the latter having a high tendency to polymerization [23], whereas others belong to the albumin fraction which also constitutes the protein isolate. As shown in Fig. 1A, the soluble fraction of AI pH8-lowIS (S) presents a polypeptide profile similar to that of total proteins (T) of the isolate, although the electrophoretic pattern of the latter exhibits a higher number of aggregated proteins unable to enter the gel. The insoluble fraction (I) exhibits a lower content of 7S globulin polypeptides of 66, 43 and 16 kDa [24], which would remain mostly in the soluble fraction.

The electrophoretic pattern of AI pH2 differs from that described for AI pH8. A much lower amount of aggregates (proteins that cannot enter the gel) is observed in the absence of ME (Fig. 1A). The patterns of total proteins (T) and the soluble fraction (S) are very similar to each other, whereas the insoluble fraction (I) differs more. The latter presents bands of molecular mass around 66, 43, 25 and 21 kDa, whereas some polypeptides of lower molecular weight are present in a lower proportion than in the total and soluble fractions. The 7S globulin, constituted by 66 kDa and 43 kDa polypeptides [24], among others, is insoluble at this pH.

While bands corresponding to P54 and to the AB subunits are virtually undetectable in the absence of ME, they appear in the electrophoretic pattern upon treatment with the reducing agent (Fig. 1B), yielding the 54 kDa polypeptide of P54 and the A and B polypeptides resulting from the cleavage of the AB subunit, thus indicating that both subunits were present in the aggregates. At high ionic strength (Fig. 1C and D) the electrophoretic patterns were less defined. The fraction soluble at pH 2 was formed by low molecular mass polypeptides, whereas the insoluble and total fraction contained the peptides that constitute the isolate. At high ionic strength and pH 8 it was observed that, similar to that described for low ionic strength, the 66 and 43 kDa peptides from 7S globulin are preferentially located in the soluble fraction.

Previous results from our laboratory indicate that the amaranth protein isolate contains an aspartic protease which is present in the seeds and that is active at pH 2.0 [25]. The presence of several low molecular mass peptides in the electrophoretic patterns, constituting the total fraction and the soluble fraction mainly at low ionic strength and the soluble fraction at high ionic strength, could result from the dissociation of amaranth proteins due to acid pH or to the action of such protease.

In order to determine the particle size distribution in soluble fractions of AI pH2-highIS, AI pH8-highIS, AI pH2-lowIS and AI pH8-lowIS the particle size distributions were analyzed (Fig. 2). Results revealed bimodal distributions with two definite populations, 1–10 nm (I) and 10–200 nm (II). Hydrodynamic ratios of both populations at pH 8 (Fig. 2A) are greater than those at pH 2 (Fig. 2B). At both pHs a left shift of both populations and the relative enrichment in particles of lower hydrodynamic ratios were observed the

Author's personal copy

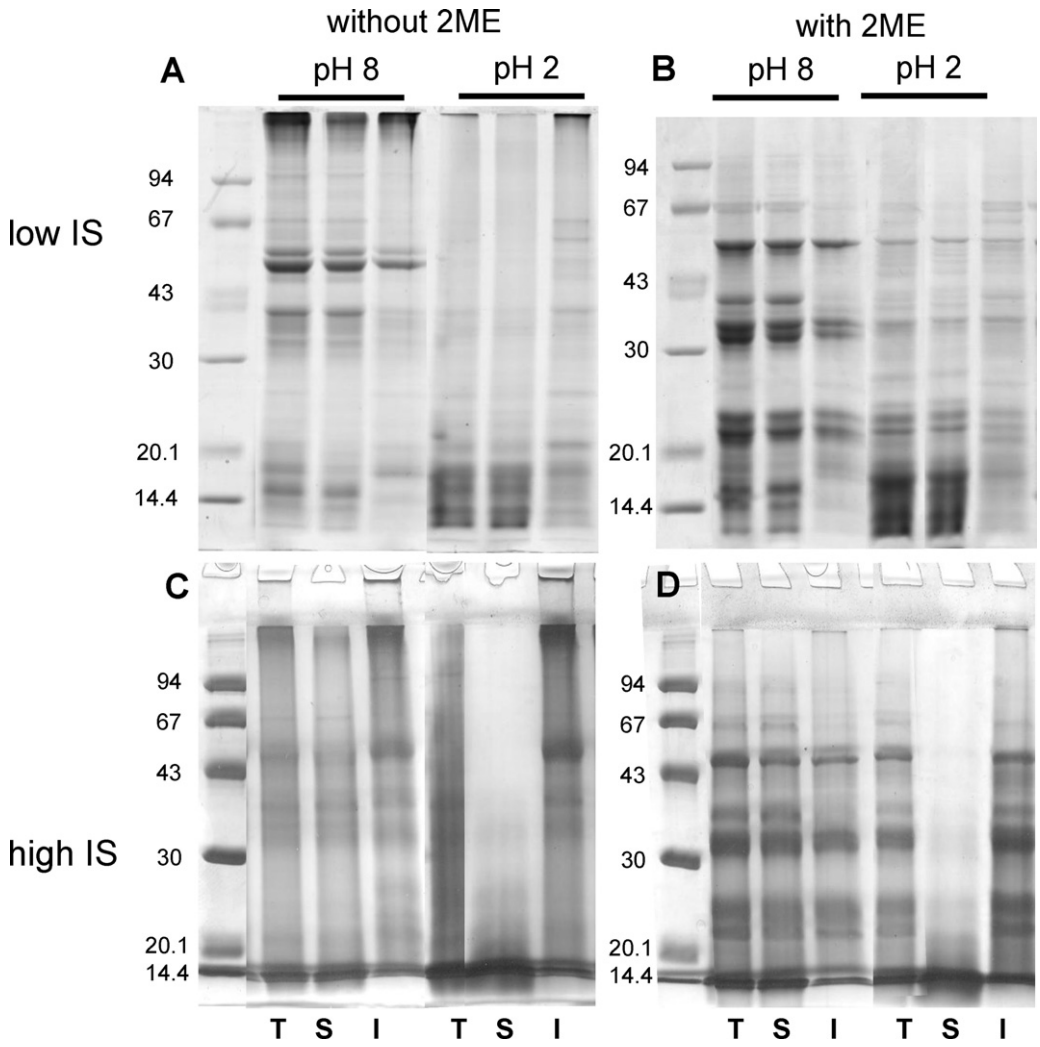

Fig. 1. Electrophoretical patterns of amaranth isolates in denaturing (A and C) and reducing denaturing (B and D) conditions. T: total protein; S: soluble protein; I: insoluble protein.

ionic strength was increased. At pH 8 and μ 0.06 (Fig. 2A), population I represents the 56% of the mass (mode 7.4 nm) while the population II represents the remaining 45% (mode 60 nm). In the case of AI pH8-highIS, was detected a relative increase of the first population (78%, mode 5.8 nm) at the expense of the second one (22%, mode 61 nm). At pH 2 and μ 0.06 (Fig. 2B) the distribution was as follows: 69% of the soluble protein mass belongs to the II population (mode 37.5 nm) and 31% to the population of lower particle size (mode 4.2 nm). As the ionic strength increases, thus promoting the establishment of hydrophobic interactions, a shift of both populations to smaller sizes was detected, with a relative mass increase in the first population (from 31% to 49%, mode 2.8 nm) as compared to the second population (from 69% to 51%, mode 32 nm). It is important to bear in mind that the increase of the ionic strength causes a loss of solubility, an effect discussed below, where a significant fraction of the proteins become part of the insoluble fraction, while the soluble fraction is enriched in smaller particles. We consider that in all samples the population II is formed by aggregates, since a protein like 11S globulin, 300–360 kDa [26], constituted by 2500–3000 aminoacids, would have a hydrodynamic radius between 4.6 and 5 nm (http://www.calctool.org/CALC/prof/bio/protein_length) while the population I corresponding to AI pH2-highIS would be formed by dissociated molecules with a hydrodynamic radius lower than 5 nm and the population I of the rest of the sample by individual molecules.

The soluble fractions of amaranth protein isolates were analyzed by circular dichroism. Fig. 2C depicts the spectra of AI pH2-highIS, AI pH8-highIS, AI pH2-lowIS and AI pH8-lowIS solutions. In the case of AI pH8-lowIS the spectrum exhibited a maximum at 190 nm, which may be associated to the folded β-sheet structure (maximum at 195 nm) [27], whereas such maximum was absent in the spectrum of AI pH2-lowIS. In addition, the minimum shifted from 208 nm for AI pH8-lowIS to 205 nm for AI pH2-lowIS, which may be attributed to an increase in random coil conformation (minimum at 198 nm) at the expense of a diminution of folded α-helix (characteristic minima at 208 and 222 nm).

The spectra of AI pH8-highIS and pH2-highIS exhibited a maximum between 195 and 200 nm, although it had lower intensity and higher wavelength than that of pH8-lowIS (190 nm). The spectra obtained for samples prepared at high ionic strength exhibited a minimum at 208 nm and a less evident one at 222 nm, suggesting the presence of α-helix structure, although the existence of random coil structure cannot be ruled out.

3.2. Functional characterization of amaranth isolates

3.2.1. Solubility

The solubility is an expression of an equilibrium state between hydrophobic and hydrophilic interactions [28]. It is a very important functional property that influences other properties like

Author's personal copy

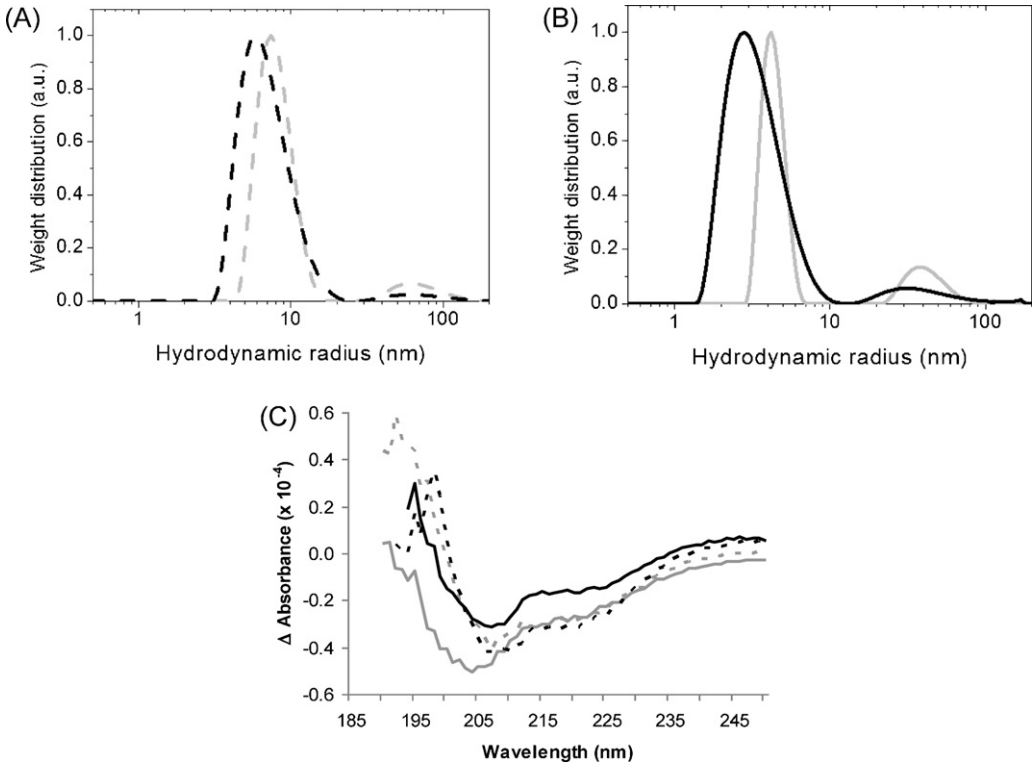

Fig. 2. Particle size distribution. (A and B) Spectrums of circular dichroism. (C) Dotted lines: protein isolates at pH8; solid lines: protein isolates at pH2; gray lines: 0.06 ionic strength; black lines: 0.5 ionic strength.

gelling, emulsifying and foaming [29]. It is known that the solubility of proteins is a function of pH, generally being minimum at the isoelectric point. Amaranth proteins have isoelectric points in the pH range: 4–6.

As shown in Table 1, the solubility of amaranth proteins was also affected by pH and ionic strength under the conditions used in this study. Amaranth proteins exhibited a relatively low solubility at pH 8, which diminished by 15.7% with the increase of ionic strength. Results obtained for samples at pH 2 indicate that, at low ionic strength, proteins are more soluble than at pH 8, becoming much more insoluble with the increase of ionic strength (solubility diminished by 70.9%). At low ionic strength and pH acid, although the proteins are unfolded, the net positive charge of the molecules allows repulsive electrostatic forces that favor a high solubility. The variation of solubility with ionic strength correlates with an increasing population of smaller particles discussed previously.

The decrease in solubility induced by salts is quantitatively more important at pH 2, probably due to an easier establishment of hydrophobic interactions between dissociated and/or unstructured peptides, or peptides hydrolyzed by the action of the protease, or those presenting a combination of the three characteristics, as described by González-Pérez et al. [30] for the denatured sunflower helianthinin.

3.2.2. *Diffusion and adsorption – rearrangement of proteins at the air:water interface*

The adsorption of proteins to the interface can be separated in different steps: diffusion, adsorption (penetration and anchoring) and rearrangement, all thermodynamically favorable. Amaranth proteins presented a different behavior in the air:water interface depending on the conditions of the assay. Fig. 3 depicts the variation of surface tension in such interface as a function of time for solutions of amaranth proteins of different protein concentration, pH and ionic strength. At low concentration of proteins in the bulk solution, adsorption at the interface depends on the diffusion process. Under this conditions (0.001 and 0.01 mg/ml protein concentration) the change of surface tension with time for all the solutions was relatively small and may be divided into two phases, a first one characterized by a constant interfacial tension and a second one presenting a relatively slow decrease of this parameter. This behavior was analyzed using the Ward and Torday's modified equation [19] and calculating the lag time and diffusion constant values, k_{diff} (Table 2).

In the case of AI pH8-lowIS and AI pH8-highIS the induction time was 21.7–21.3 min at 0.001 g/l of protein and decreased to 4.1–2.7 min with increases of the protein concentration ten times. While at pH2-lowIS and 0.001 g/l of protein the induction time detected was the greater (64.3 min); this time decreased markedly with the increase of protein concentration or the ionic strength at the two protein concentrations assayed. These results agree with those obtained by Rodriguez Patino et al. [31] for soybean beta-conglycinin and glycinin at 0.001 g/l, μ 0.05, pH 2.0 and 8.0.

Lowering the pH and increasing the ionic strength of the solution significantly diminished the induction time. This result may be attributed to the presence of a larger proportion of smaller particles and high positive charge of the protein molecules, and consequently to the lower probability of adsorption of the particles at the interface and increased energy barrier that must be overcome the protein molecules to adsorb to the water:air interface [32].

In Table 2, it can also be observed that in the case of AI pH8-lowIS the value of the k_{diff} increases with increasing concentrations of the solution, suggesting a faster adsorption. These values are not modified with the increasing of the ionic strength (AI pH8-highIS). When pH is reduced to 2.0 and the ionic strength is kept low (AI pH2-lowIS), k_{diff} values are slightly higher than those measured at pH 8.0, implying a positive effect of pH on the adsorption of amaranth proteins. The increase in ionic strength (AI pH2-highIS)

Author's personal copy

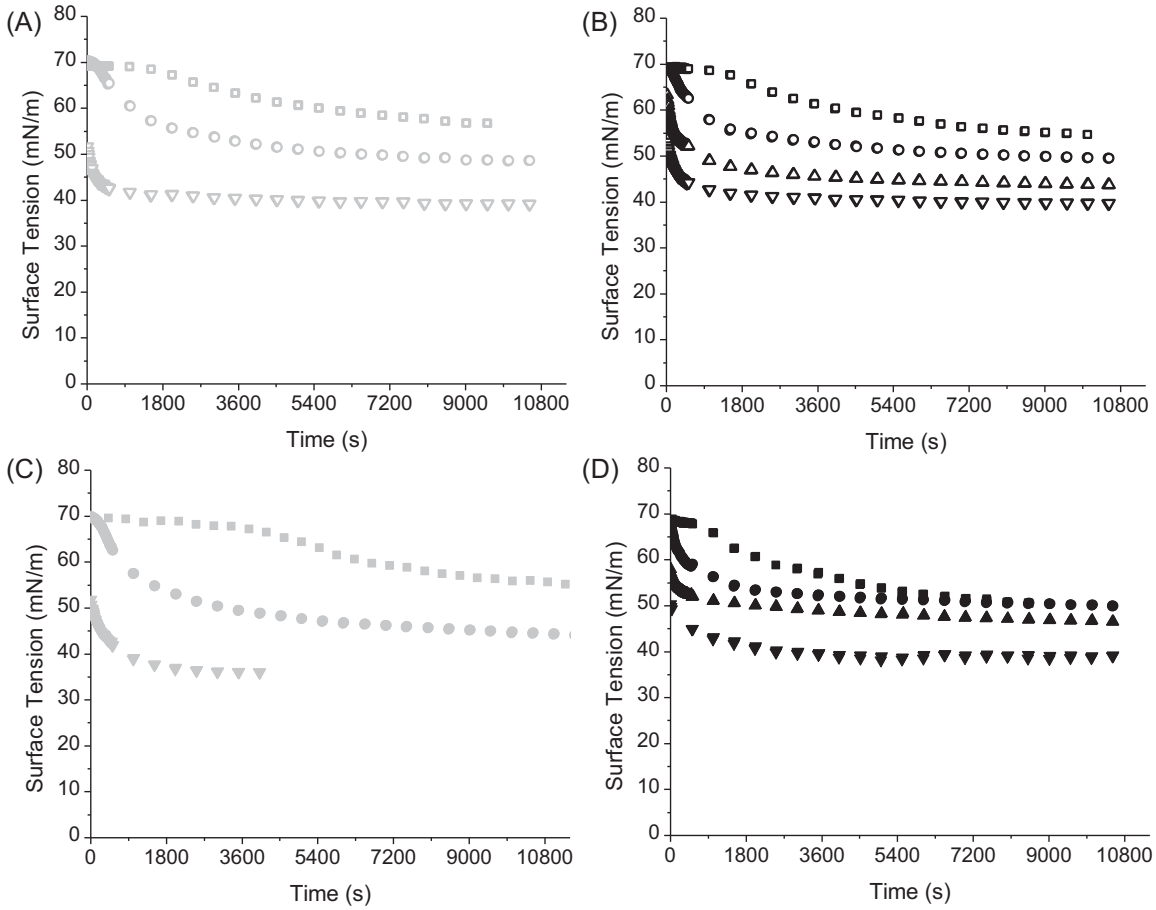

Fig. 3. Surface tension as a function of time. Effect of protein concentration. Square symbols: 0.001 mg/ml; circles: 0.01 mg/ml; triangle: 0.1 mg/ml; upside down triangle: 1 mg/ml. Panels A and B: protein isolates at pH 8. Panels C and D: protein isolates at pH 2. Gray symbols: 0.06 ionic strength; black symbols: 0.5 ionic strength. Typical points of one of the triplicates carried out are shown. The points of each assay overlapped.

increased markedly the k_{diff} value as compared to values measured at pH 8.0, increase that could be attributed to the smaller size of the protein molecules.

Under the different conditions assayed, the increase of the diffusion rate was related to a lower induction time, probably due to a variation in the particle size and flexibility of molecules. According to our results, in order to favor the diffusion of the particles at the interface and the rapid reduction in interfacial tension, the following conditions must be met: more protein, less surface charge (due to the higher ionic strength), smaller size and greater degree of unfolding (due to acid pH).

At higher concentrations (1 mg/ml) protein diffusion no longer constituted a limitation for the adsorption process while other processes started to influence it, such as penetration and anchorage – usually included in the adsorption term – and unfolding and rearrangement of the protein in the air:water interface. At 1 mg/ml of protein in the solution the variation of interfacial tension over time is much more pronounced (Fig. 3) observing a first very rapid phase followed by a slower one until reaching a constant value that marks the attainment of equilibrium.

Amaranth protein adsorption and rearrangement in the air:water interface were estimated applying the model of Panizzolo [20] to the curves shown in Fig. 3, allowing to calculate the relative weight of adsorption and rearrangement processes through the estimation of k_a, k_r, γ_a and γ_r. The results obtained are shown in Table 3. The calculated k_a values confirmed that proteins at pH 2.0 are adsorbed faster than those at pH 8.0, at both ionic strength assayed. These results are consistent with the values of

Table 2
Lag time, diffusion constant (k_{diff}), and diffusion time calculated by Ward and Torday modified equation.

Sample	Concentration (mg/ml)	Lag period (min)	k_{diff} (mN/m$\sqrt{t}$)	Diffusion time (min)
AI pH8-lowIS	0.001	21.7	1.43 (0.997)	88.5
	0.01	4.1	3.13 (0.992)	21.7
AI pH8-highIS	0.001	21.3	1.45 (0.996)	99.0
	0.01	2.7	2.97 (0.993)	22.6
AI pH2-lowIS	0.001	64.3	1.52 (0.991)	103.0
	0.01	3.7	3.74 (0.994)	15.3
AI pH2-highIS	0.001	12.2	1.85 (0.995)	87.8
	0.01	0.1	5.61 (0.998)	2.6

Data in parenthesis: correlation coefficient.

Author's personal copy

Table 3
Adsorption and rearrangement constants (k_a and k_r), amplitude of the process (γ_a and γ_r) and interfacial tension at short time (γ(3 s)) and long time ($\gamma(\infty)$) estimated applying the Panizzolo model. Values ± standard error, $p < 0.05$.

Sample	γ_a	k_a	γ_r	k_r	γ(3 s)	$\gamma(\infty)$
AI pH8-lowIS	14.4 ± 0.6	0.111 ± 0.012	6.87 ± 0.66	0.00712 ± 0.0015	67.75 ± 0.65	50.72 ± 0.18
AI pH8-highIS	17.1 ± 1.3	0.161 ± 0.021	8.10 ± 0.68	0.0093 ± 0.0015	65.22 ± 0.97	46.80 ± 0.18
AI pH2-lowIS	13.9 ± 1.1	0.241 ± 0.021	4.26 ± 0.23	0.0100 ± 0.0010	64.71 ± 0.62	53.79 ± 0.22
AI pH2-highIS	17.3 ± 1.6	0.359 ± 0.027	3.71 ± 0.16	0.01019 ± 0.00088	60.47 ± 0.41	50.98 ± 0.16

adsorption rate and particle size distribution determined and which are dependent on the ionic strenght and pH of the solutions. The smaller the particle size the greater the interfacial entropy, which favors the penetration and anchoring at the interface [33]. The evaluation of the amplitude of the process, γ_a, allowed us to estimate the reduction of the surface free energy caused by the adsorbed protein. No significant differences in the decrease of the surface tension were detected at pH 2.0 and 8.0, however, a greater decrease was detected upon increasing the ionic strength, probably due to the reduction of the repulsion between proteins. This phenomenon would facilitate a better rearrangement in the interface [34].

The calculated k_r values were at least an order of magnitude lower than those for the adsorption process. Modification of the pH and ionic strength of the solution did not change the k_r determined. The amplitude of the decrease, γ_r, in surface tension due to rearrangement of the protein molecule at the interface was lower than that for its adsorption. The values obtained for AI pH8-low and highIS were 6.9 and 8.1 mN/m, respectively. The decrease of pH at both ionic strengths (AI pH2-lowIS and AI pH2-highIS) produced a significant decrease in the extent of the rearrangement (4.3 and 3.7 mN/m, respectively). These results showed that, the rearrangement in the interface predominates at pH 8.0 probably due to the fact that proteins under these conditions exhibit a more native conformation and, therefore, need more time to unfold at the interface. At both pH values an increase of ionic strength increased adsorption magnitude and velocity.

3.2.3. Foaming properties

The rate of liquid incorporation to the foam (v_o) is commonly used as a measure of the foaming capacity of proteins, so that proteins with faster liquid incorporation are considered better foaming proteins. In the present study v_o was higher for AI pH2-lowIS than for AI pH8-lowIS, and it was higher for samples of high ionic strength (AI pH2-highIS and AI pH8-highIS) (Fig. 4B, $p < 0.05$).

When foams are obtained by the sparging method, proteins yielding a greater foam volume (maximal foam volume, VEmax) are considered to have better foaming properties. Among the studied samples, foams prepared in all conditions exhibited the same VEmax values (data not shown).

Foam density was calculated as the ratio between the mass of liquid incorporated to the foam and the foam volume (Fig. 4A). The most dense foams were those prepared with AI pH 2, regardless of the ionic strength value ($p < 0.05$). For foams obtained by sparging, the foaming capacity of a protein increases with the foam density [20], thus giving further support to the conclusions drawn from v_o results. More dense foams could contain smaller bubbles, thus generating a larger interfacial surface, created by the protein solution during sparging, and thus a higher liquid volume for the same foam volume. The fact the difference in density may not be reflected in differences in the size of bubbles but in the thickness of lamella cannot be ruled out. A thicker lamella could originate more dense foams regardless of the bubble radius.

Foams are denser at pH 2, a value at which the net charge is positive [12], thus producing a large repulsion between proteins in the interface and a greater lamellar thickness. Images of the foams obtained are shown in Fig. 4C. It can be observed that foams obtained at lowIS had a more homogeneous distribution of bubbles size than those obtained at highIS. There were no significant visual differences between foams obtained at alkaline or acidic pH. In addition, bubbles were smaller at a higher ionic strength.

In order to compare the influence of the insoluble protein fraction on the foam formation capacity of the samples assayed, experiments were performed with the total protein (soluble protein + insoluble protein) dispersions. The results obtained showed that the foams formed with the total fraction incorporated less liquid and reached less volume than those corresponding to the foams of the soluble fraction, with the exception of the sample AI pH2-lowIS, which showed no differences with the soluble fraction. Moreover these foams were less dense, with bubbles larger and less homogeneous than foams formed with the respective soluble fractions, except for the case of AI pH8-highIS that showed no differences (data not shown).

Finally we examined the increase in protein concentration of both the soluble fraction and the overall dispersion; to this end, the AI pH2-highIS sample was selected. For the soluble fraction a significant increase in foam density with increasing protein concentration was observed. Foams formed in both cases were similar, with no significant differences between the measured parameters, suggesting that the insoluble fraction of the samples tested did not affect the characteristics of the foams (Table 4).

3.3. Discussion

The adsorption of proteins may be related with their surface and structural characteristics, which determine their affinity for the air:water interface.

The results discussed above show that amaranth proteins are modified at acid pH by dissociation/association reactions and, according to the results of Ventureira et al. [25], by the action of an endogenous protease that activates in the assay conditions producing the partial hydrolysis of some amaranth polypeptides. Such modifications lead to a reduction of the molecular size of amaranth proteins, particularly those that remain soluble, and also to a greater flexibility, these characteristics probably being responsible for the difference in adsorption velocity detected under acid pH conditions as compared to alkaline pH.

In addition, the increase in ionic strength produced a very pronounced reduction of solubility, especially for amaranth proteins at acid pH. This decrease may be attributed to the masking of surface charges, which reduces the repulsion between polypeptides and thus favors protein aggregation and the consequent precipitation. Results obtained by electrophoresis (Fig. 1), circular dichroism and analysis of particle size distribution (Fig. 2) show that proteins that became insoluble at pH 2 were the larger ones, specially those polypeptides of 66, 45, 25 and 21 kDa at lowIS and polypeptides belonging to 7S, 11S and globulin P at highIS (Fig. 1) and those with a disordered structure. Therefore, protein solutions of AI pH2-highIS would be enriched in soluble protein structures of smaller size and greater structural degree. Such proteins were the ones with best tensioactive properties, which were reflected not only in the decrease of interfacial tension but also in the increase of foaming velocity.

Author's personal copy

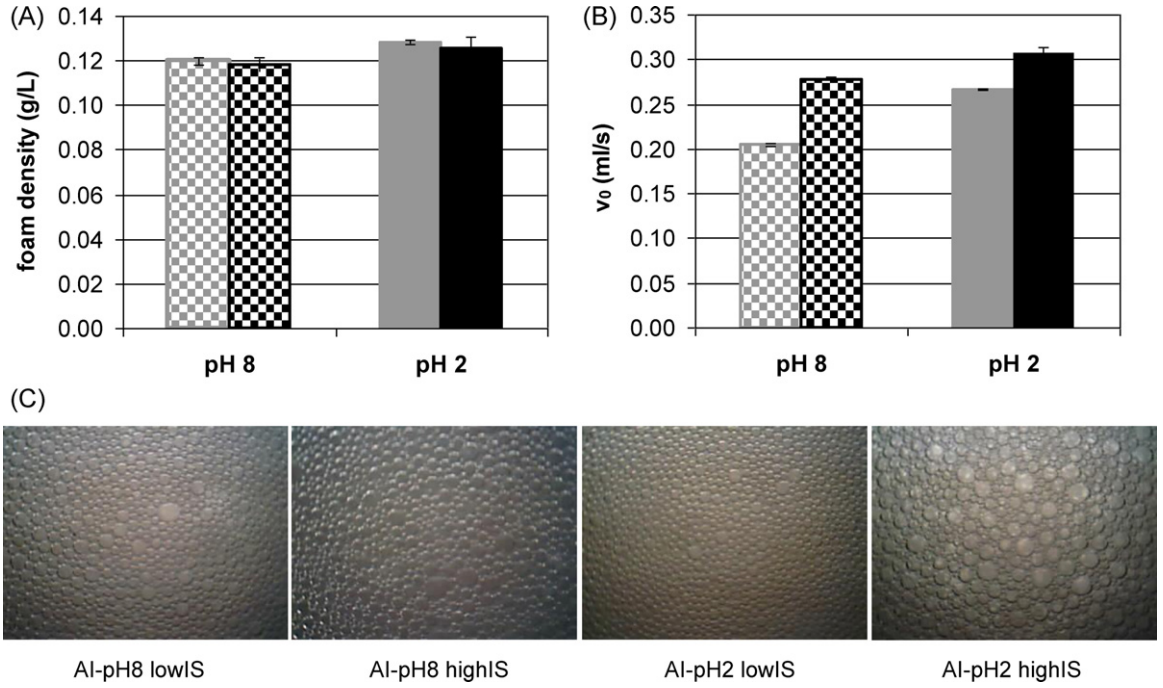

Fig. 4. Foaming properties. Panel A: density of foams. Panel B: rate of liquid incorporation, v_0. Hatched bars: proteins at pH 8; solid bars: proteins at pH 2; gray bars: 0.06 ionic strength; black bars: 0.5 ionic strength. Panel C: foam's images at different conditions. Error bars indicate standard deviation of at least three assays.

Table 4
Foam formation parameters (v_0 and foam density) of solutions and dispersions of amaranth proteins.

Soluble protein concentration	v_0 (ml/s)		Foam density (g/l)	
	Protein solution	Protein dispersion	Protein solution	Protein dispersion
0.25 mg/ml	0.268[a]	0.298[b*]	0.1130[a]	0.1181[ab*]
1 mg/ml	0.305[b]	0.298[b**]	0.1255[b]	0.1224[b**]

In each column different letters indicate significantly different values ($p < 0.05$).
* Protein dispersion contains 0.25 mg/ml of soluble protein and 0.75 mg/ml of insoluble protein.
** Protein dispersion contains 1 mg/ml of soluble protein and 3 mg/ml of insoluble protein.

The lag period was reduced at pH2-highIS as compared to the other conditions assayed (pH2-lowIS, pH8-highIS and pH8-lowIS), and the adsorption process was enhanced.

At concentrations at which adsorption was limited by diffusion (0.001 and 0.01 g/l), the value of the diffusion coefficient increased with increasing concentrations, as expected. The highest value was obtained at pH2-highIS, without interaction between both factors. The same tendency was observed regarding adsorption. Both phenomena, diffusion and adsorption, were favored by the presence of smaller, more hydrophobic and flexible particles, which benefit the process impaired by the net positive charge conditions.

The results obtained showed that the rate of liquid incorporation to the foam, v_0, was greater for AI pH2-lowIS than for AI pH8-lowIS, and that such velocity was increased in samples of high ionic strength (AI pH2-highIS and AI pH8-highIS). The rate constant of protein adsorption to the interface drives the increment of surface pressure in the short term; in turn, such increment is necessary to enhance the increase of interfacial surface and foam formation. Fig. 5 shows the existence of a relationship between the increase of surface pressure and liquid incorporation to the foam, v_0. According to Prins et al. [35] a higher surface pressure at the time of bubble formation should lead to a lower bubble radius. The experimental measures performed in the present study did not allow detecting significant differences between the different samples. Nevertheless, more dense foams were obtained at pH 2 than at pH 8, which may be attributed to the higher net charge density that a thicker lamella would support by repulsion of both interfaces.

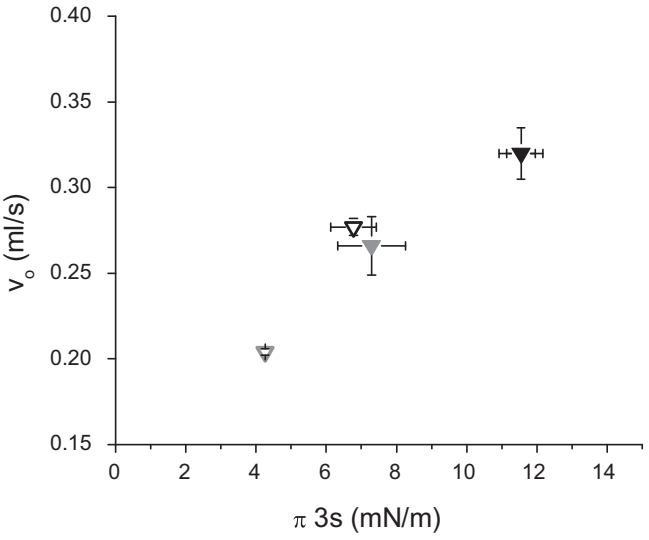

Fig. 5. Relationship between maximum rate of liquid incorporation to the foam, v_0, and surface pressure at time 3 s. Protein solutions (1 mg/ml): empty gray triangle: pH 8-lowIS; empty black triangle: pH 8-highIS; solid gray triangle: pH 2-lowIS; and solid black triangle: pH 2-highIS. Low and high ionic strength: 0.06 and 0.5 respectively. Error bars in y axis, v_0, indicate standard deviation of at least three assays. Error bars in x axis, π_{3s}, indicate standard error of at least three determinations.

Author's personal copy

In conclusion, treatment at pH 2, together with the increase of ionic strength of the medium, substantially improves the foaming properties of amaranth proteins, opening new ways for their use as functional ingredient. These findings would also represent an extra contribution to the health of consumers, since the proteins of amaranth contain encrypted sequences with demonstrated biological activities [6,7].

References

[1] H. Aiking, Trends Food Sci. Technol. 22 (2011) 112.
[2] O.L. Tavano, S.I. Da Silva Jr., A. Damonte, V.A. Neves, J. Agric. Food Chem. 56 (2008) 11006.
[3] B. Salcedo-Chávez, J.A. Osuna-Castro, F. Guevara-Lara, J. Dominguez-Domínguez, O. Paredes-López, J. Agric. Food Chem. 50 (2002) 6515.
[4] S.H. Guzmán-Maldonado, O. Paredes-López, in: J.R. Whitaker, F. Shahidi, A. López-Munguia, R.Y. Yada, G. Fuller (Eds.), Functional Properties of Proteins and Lipids, Am. Chem. Soc., Washington, DC, 1998, p. 66.
[5] S.N. Thanapornpoonpong, S. Vearasilp, E. Pawelsik, S. Gorinstein, J. Agric. Food Chem. 56 (2008) 11464.
[6] M.C. Orsini Delgado, V.A. Tironi, M.C. Añón, LWT-Food Sci. Technol. 44 (2011) 1752.
[7] D.A. Barrio, M.C. Añón, Eur. J. Nutr. 49 (2010) 73.
[8] S. Damodaran, A. Paraf, Food Proteins and their Application, Dekker, New York, 1997.
[9] E. Dickinson, Colloids Surf. B: Biointerfaces 20 (2001) 197.
[10] D.J. McClements, Food Emulsions: Principles, Practice and Technics, CRC Press, Boca Raton, FL, 2000.
[11] V.P. Ruiz-Henestrosa, C. Carrera Sánchez, M.M. Yust Escobar, J.J. Pedroche Jiménez, F. Millán Rodríguez, J.M. Rodríguez Patino, Colloids Surf. A: Physicochem. Eng. Aspects 309 (2007) 202.
[12] J.L. Ventureira, A.J. Bolontrade, F. Speroni, E. David-Briand, A.A. Scilingo, M.-H. Ropers, F. Boury, M.C. Añón, M. Anton, LWT 45 (2012) 1.
[13] AOAC (Association of Official Analytical Chemists Inc.), in: S. Williams (Ed.), Official Methods of Analysis, 14th ed., AOAC, Arlington, VA, 1984, Method 2057, p. 16.
[14] M. Segura-Nieto, A.P. Barba de la Rosa, O. Paredes López, in: O. Paredes-López (Ed.), Amaranth: Biology, Chemistry and Technology, CRC, Boca Raton, 1994, p. 75.
[15] E.N. Martínez, M.C. Añón, J. Agric. Food Chem. 44 (1996) 2523.
[16] E.N. Martínez, O.F. Castellani, M.C. Añón, J. Agric. Food Chem. 45 (1997) 3832.
[17] O.H. Lowry, N.J. Rosebrough, A.L. Farr, R.J. Randall, J. Biol. Chem. 193 (1951) 265.
[18] S.W. Provencher, Comput. Phys. Commun. 27 (1982) 213.
[19] J.M. Rodríguez Patino, M.R. Rodríguez Niño, Colloids Surf. B: Biointerfaces 15 (1999) 235.
[20] L.A. Panizzolo, Modificación de proteínas por vía enzimática, Análisis de la relación estructura-funcionalidad de los productos de hidrólisis, PhD Thesis, Facultad de Química, Universidad de la República, Uruguay, 2005.
[21] W. Loisel, J. Gueguén, Y. Popineau, in: K.D. Schwenke, R. Mothes (Eds.), Food Proteins: Structure and Functionality, VCH, Weinheim, Germany, 1993, p. 320.
[22] S.D. Arntfield, E.D. Murray, Can. Inst. Food Sci. Technol. J. 14 (1981) 289.
[23] O.F. Castellani, E.N. Martínez, M.C. Añón, J. Agric. Food Chem. 47 (1999) 3001.
[24] Quiroga, E.N. Martínez, H. Rogniaux, A. Geairon, M.C. Añón, J. Agric. Food Chem. 58 (2010) 12957.
[25] J.L. Ventureira, E.N. Martínez, M.C. Añón, Food Hydrocolloids 29 (2012) 272.
[26] M.F. Marcone, R.Y. Yada, Food Chem. 61 (1998) 319.
[27] N. Greenfield, G.D. Fasman, Biochemistry 8 (1969) 4108.
[28] S. Damodaran, Interrelationship of molecular and functional properties of food proteins, in: J.E. Kinsella, W.G. Soucie (Eds.), Food Proteins, The American Oil Chemists Society, Champaign, IL, 1989, p. 21.
[29] P.J. Halling, CRC Crit. Rev. Food Sci. Nutr. 13 (1981) 155.
[30] S. González-Pérez, J.M. Vereijken, K.B. Merck, G.A. Van Koningsveld, H. Gruppen, A.G.J. Voragen, J. Agric. Food Chem. 52 (2004) 6770.
[31] J.M. Rodriguez Patino, C. Carrera Sánchez, S.E. Molina Ortiz, M.A. Rodríguez Niño, M.C. Añón, Ind. Eng. Chem. Res. 43 (2004) 1681.
[32] T. Sengupta, L. Razumovsky, S. Damodaran, Langmuir 15 (1999) 6991.
[33] A.R. Mackie, F.A. Husband, C. Holt, P.J. Wilde, Int. J. Food Sci. Technol. 34 (1999) 509.
[34] R. Miller, V.B. Fainerman, A.V. Makievski, J. Krägel, D.O. Grigoriev, V.N. Kazakov, O.V. Sinyachenko, Adv. Colloid Interface Sci. 86 (2000) 39.
[35] A. Prins, in: E. Dickinson, G. Stainsby (Eds.), Advances in Foams Emulsions and Foams, Elsevier Applied Science, London, 1988, p. 91.